

Contents list available at CBIORE journal website

### **International Journal of Renewable Energy Development**

Journal homepage: https://ijred.cbiore.id



**Research Article** 

# Natural pigment-based dye-sensitized solar cells utilizing *Caulerpa* racemose and *Gymnogongrus flabelliformis* as photosensitizers

Semuel Unwakoly<sup>a.b</sup>, Liliasari<sup>a</sup>, Sri Hartati<sup>c</sup>, Heli Siti H. Munawaroh<sup>a</sup>, Arramel<sup>c</sup>, Prima Fitri Rusliani<sup>d</sup>, Eka Cahya Prima<sup>a</sup>

**Abstract**. This research examines natural dyes' chemical and physical characteristics for potential use in dye-sensitized solar cells (DSSCs). Chlorophyll pigments were extracted from two macroalgae species, *Caulerpa racemosa* and *Gymnogongrus flabelliformis*, and analyzed using absorbance spectroscopy, band gap energy calculations, and dye-sensitized solar cell performance evaluation. Fourier Transform Infrared (FTIR) characterisation was used to identify the pigments contained in the dye. The absorbance spectra of chlorophyll pigments extracted from both macroalgae species showed broad peaks at 400–800 nm wavelengths, with *Gymnogongrus flabelliformis* showing the highest absorbance peak at 403 nm. The redox potential analysis for both macroalgae species showed energy gaps (HOMO/LUMO) of 1.3 eV, 1.4 eV, 2.3 eV, and 2.4 eV, respectively, indicating that these natural dyes are suitable for use in DSSC applications. DSSC devices were fabricated using components such as liquid electrolyte, mesoporous titanium dioxide (TiO<sub>2</sub>) photoelectrode, reduced graphene oxide (rGO) as counter electrode, and ITO glass as conductive substrate. Meanwhile, to evaluate how well the photovoltaic system worked, we looked at short-circuit current density (*Jsc*), open circuit voltage (*Voc*), fill factor (*FF*), and overall photoelectric conversion efficiency ( $\eta$ ). The results showed that the highest performance for *Gymnogongrus flabelliformis* was *Jsc* 0.041 mA/cm², *Voc* 0.28 V, *FF* 0.239, and  $\eta$  0.020%, while the highest performance of *Caulerpa racemosa* was *Jsc* 0.023 mA/cm², *Voc* 0.46 V, *FF* 0.244, and  $\eta$  0.019%. These findings indicate the potential for using and developing natural dyes derived from these two macroalgae species in DSSC technology. This research offers insight into the feasibility of marine-derived pigments as a sustainable and environmentally friendly alternative for photovoltaic applications.

Keywords: DSSC, natural pigment, Caulerpa racemose, Gymnogongrus flabelliformis, Photosensitizers



@ The author(s). Published by CBIORE. This is an open-access article under the CC BY-SA license.
[http://creativecommons.org/licenses/by-sa/4.0/).

Received: 20th January 2025; Revised:17th March 2025; Accepted: 16th April 2025; Available online: 24th April 2025

#### 1. Introduction

The depletion of fossil fuels such as oil, coal, and natural gas, resulting in the release of harmful exhaust gases, including carbon dioxide, sulfur dioxide, and carbon monoxide, which contribute to air pollution and global warming (Chen, Wang, Chen, & Chen, 2012; A. Kumar & Kandpal, 2007). This situation highlights the urgent need for renewable energy sources that are affordable and environmentally friendly (Ciani, Catelani, Carnevale, Donati, & Bruzzi, 2014). Dye-sensitized solar cells (DSSCs) are an inexpensive, easily manufactured, clean, and sustainable renewable energy technology that is currently under development and generating significant interest. As thirdgeneration solar cells, DSSCs offer an efficient mechanism for light absorption and conversion into electrical energy compared earlier configurations. This technology comprises semiconductor anodes, photosensitizers, redox electrolytes, and photocathode nanostructures (Cui et al., 2021; Ferreira et al., 2020). In DSSCs, light absorption and electrical charge separation occur through distinct processes: dye molecules

absorb light, while nanocrystalline inorganic semiconductors with wide band gaps, such as TiO<sub>2</sub>, facilitate charge separation.

The dye-sensitizer agent is a crucial component of DSSC performance and is the cell configuration's core element. Natural dyes offer several advantages in DSSCs, including abundant availability, cost-effectiveness, biodegradability, nontoxicity, and straightforward synthesis procedures. Various natural dyes derived from plants and algae—such as anthocyanin's, betalains, carotenoids, xanthophyll's, and chlorophylls—have been employed in DSSCs, demonstrating varying levels of efficiency (Erdogdu, Atilgan, Erdogdu, & Yildiz, 2024; Hao, Wu, Huang, & Lin, 2006; Iqbal, Ali, & Khan, 2019). Plant pigmentation results from the interaction between the electronic configuration of the pigment and solar radiation, which modulates the wavelength of light that is either reflected or transmitted by plant tissue (Davies, 2004).

Macroalgae, a type of marine plant predominantly found in shallow water environments, have attracted significant interest in DSSC production due to the high concentration of photosynthetic pigments, making it a promising source of

<sup>&</sup>lt;sup>a</sup>Natural Science Education, Mathematics and Natural Science Education Faculty, Indonesia University of Education, Indonesia

 $<sup>^</sup>b$ Chemistry Education Study Program, Faculty of Education and Teacher Training, Pattimura University, Indonesia

<sup>&</sup>lt;sup>c</sup>Center of Excellence Applied Physics and Chemistry, Nano Center Indonesia, Indonesia

 $<sup>^</sup>d$ Solar Energy Material Laboratory, Mathematics and Natural Science Education Faculty, Indonesia University of Education, Indonesia

natural colorants for such applications. Chlorophyll, one of the key pigments in macroalgae, is valuable for spectroscopic investigations and practical applications due to its ability to interact with visible electromagnetic radiation. (Mandal & Dutta, 2020). The primary distinction between chlorophyll b and chlorophyll a lies in the presence of an aldehyde substituent (-CHO) in chlorophyll b, replacing the methyl group (-CH<sub>3</sub>) found in chlorophyll a (Grimm, Porra, Rüdiger, & Scheer, 2006). Chlorophyll c is indicated by the carboxyl group on its terminal moiety, which is linked to the porphyrin macrocycle through a pair of conjugated double bonds. The configuration facilitates photoinduced electron transfer from the porphyrin macrocycle to the semiconductor electrode near the seaweed pigment (Wang, Zhan, Maoka, Wada, & Koyama, 2007).

Several studies have reported varying performance levels when different macroalgae species are used in DSSC fabrication. Wang et al. studied the efficiency of TiO2-based solar cells in converting light to electricity using two types of chlorophyll c pigments from U. pinnatifida (c1 and c2) and their oxidized forms (c1' and c2'). The results were as follows: c2 (4.6%), c1 (3.4%), c2' (2.6%), and c1' (2.5%) (Wang et al., 2007). Calogero et al. reported a performance productivity of 0.178% and a fill factor of 0.69% using chlorophyll pigments from U. pinnatifida (Calogero et al., 2014). Meanwhile, Minicante et al. achieved an efficiency of 0.36% and a fill factor of 0.71% with chlorophyll extract from *U. pinnatifida* (Minicante et al., 2016). In another study, sensitization with chlorophyll extract from Enteromorpha intestinalis seaweed produced a photoconversion effectiveness of 0.13% with a fill factor of 0.46 (Dumbrava, Lungu, & Ion, 2016).

A semiconductor must exhibit significant porosity of ~50%, a high surface area, and a wide band gap to function effectively as a photoelectrode (Grätzel, 2001; Orona-Navar, Aguilar-Hernández, Nigam, Cerdán-Pasarán, & Ornelas-Soto, 2021). The nanocrystalline particles of the mesoporous film have to accept excited electrons from the dye to generate an electric current, which requires compatibility between their electronic characteristics and those of the sensitizer (Richhariya, Kumar, Tekasakul, & Gupta, 2017).  ${\rm TiO_2}$  is the semiconductor most used in DSSCs, although some other materials, such as ZnO and  ${\rm SnO_2}$ , can also be employed.

TiO<sub>2</sub> is the preferred material in photoelectrochemical systems due to its availability, low cost, non-toxicity, and stability at high temperatures. The excited levels of natural pigments' low-energy empty molecular orbitals (LUMO) must be compatible with the conduction band in the anatase phase (3.2 eV) to guarantee effective electron injection. According to Kumar *et al.* (2017), TiO<sub>2</sub> has a high refractive index (n = 2.5) that promotes light absorption and dispersion in semiconductor films (Kumar & Rao, 2017; Kumara, Lim, Lim, Petra, & Ekanayake, 2017; Olea, Ponce, & Sebastian, 1999). Along with the photosensitizer, the counter electrode that functions as a catalyst in the electron transfer cycle should have high electrical conductivity and rapid charge transfer performance. (Ubani *et al.*, 2016).

Platinum and carbon materials such as graphite, activated carbon, carbon nanotubes, carbon black, fullerene, and graphene are frequently applied as counter electrodes. Platinum is a standard material utilized in the DSSC fabrication because it is of outstanding quality in catalytic activity and has excellent electrolyte stability (Wu & Ma, 2014). Nevertheless, this material is limited in availability, easy to corrode by I- and I3- redox electrolytes, and expensive (Ruba *et al.*, 2021; Zhu *et al.*, 2016). These limitations allow using carbon materials such as graphene as excellent counter electrodes because it has a specific two-

dimensional honeycomb crystal structure that results in excellent chemical stability, high transmittance, and electrical conductivity (Venugopal, Krishnamoorthy, & Kim, 2013).

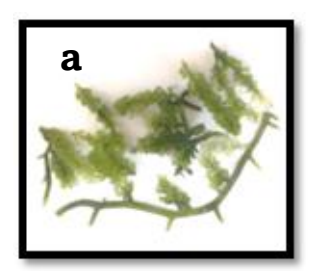
Spectroscopic techniques assessed how well the macroalgae species *Caulerpa racemosa* and *Gymnogongrus flabelliformis* perform regarding charge transfer ability, electrical properties, absorbance and adsorption, and energy efficiency. FTIR and UV-Vis spectroscopy were used to analyze the molecular vibration of the dye photosensitizer. In addition, the redox potential was evaluated using cyclic voltammetry. Specifically, gap energy, HOMO-LUMO orbitals, oxidation, and reduction potential are other components of the redox potential study. The low current density (Jsc), open circuit voltage (Voc), fill factor (FF), and power conversion efficiency ( $\eta$ ) were examined by investigating the characteristics of the J-V (Prima, Nugroho, Refantero, Panatarani, & Yuliarto, 2020).

Macroalgae species such as *Caulerpa racemosa* and *Gymnogongrus flabelliformis* can be found throughout the coastal waters of Maluku, Indonesia. (Liline, Rumahlatu, Zubaidah, Salmanu, & Sangur, 2024). Thus, it is a readily available and sustainable resource for chlorophyll extraction as an efficient natural dye for DSSCs. Although these two macroalgae species are abundant in coastal marine ecosystems, their utilization in DSSC photovoltaic technology has not been widely explored. Consequently, by integrating the advantages of local abundance, pigment characteristics, and novelty in DSSC technology, this study aims to measure the performance of chlorophyll extracts from *Caulerpa racemosa* and *Gymnogongrus flabelliformis* as sensitizers in DSSC photovoltaic technology. This research contributes to developing sustainable and efficient natural dyes for future solar cell technology.

#### 2. Materials and Methods

#### 2.1 Materials and Tools

This study used several materials, such as transparent conductive glass plate electrode from OPV-Tech (China), ethanol, and acetone from Merck (Germany), and Caulerpa racemosa (LILINE et al., 2024), as shown in Figure 1a. This green macroalgae species exhibits a naturally high population density and is widely distributed in the waters of the Kei Islands, Maluku Province, Indonesia, throughout the year. Gymnogongrus flabelliformis (LILINE et al., 2024) in Figure 1b, is a red macroalgae species that exhibits prolific growth and can be reliably observed in the waters surrounding Ambon Island, Maluku Province, Indonesia, during July each year. Additional materials included filter paper No. 102 from BKMAMLAB (China), distilled water, EL-HPE/High-Performance Electrolyte from Greatcell (Australia), Low-Temperature Thermoplastic Sealant (also from Greatcell), as well as a dark glass bottle and aluminum foil. Filter paper no. 102 from BKMAMLAB in China,



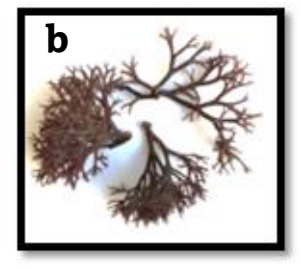


**Fig 1**. Photograph of natural dyes collected from macroalgae. (a). *Caulerpa racemosa*, (b). *Gymnogongrus flabelliformis* 

distilled water, EL-HPE/High-Performance Electrolyte from Greatcell in Australia, Low-Temperature Thermoplastic Sealant also from Greatcell, as well as a dark glass bottle, and aluminum foil.

This research utilized an ultrasonic cleaner (BAKU BK-2000), a drying oven (DHG-9053 A), a muffle furnace (SUHATHERM), a blender, and digital scales. Additional equipment included a micropipette (Accurate), a glass beaker, a measuring cup, a petri dish, a multimeter (KRISBOW KWD6-796), a magnetic stirrer (DLAB MS-H260-Pro), a spin coater (GLICHN T-108), a centrifuge (Oregon LC-04S), centrifuge tubes, a filtration buncher vacuum kit, a pH meter (IONIX pH10), a paper clip, a Fourier transform infrared spectrometer (BUNKER), a UV-Vis spectrophotometer (W&J CE ROHS UV1600PC), a DC voltage/current source monitor (ADCMT 6242), and a solar standard simulator with an AM 1.5G filter at 100 mW/cm².

#### 2.2 Chlorophyll extraction as natural dye sensitizers

Fresh Caulerpa racemosa and Gymnogongrus flabelliformis were washed seven times under running water to remove dirt and reduce salt content. They were then air-dried for 12 days until the sample weight stabilized. The dried samples were cut into small pieces, pulverized using a blender, and stored in a dry, dark, room-temperature environment for future use. Adjustments were made to the maceration method to extract chlorophyll pigments. The pigments were extracted using ethanol (96%) and acetone (96%) in a 1:5 (w/v) ratio. Each sample weighed 20 grams and was placed into four preprepared, labeled, and numbered dark bottles: Cl-01 for Caulerpa racemosa-ethanol, Cl-02 for Caulerpa racemosaacetone, Gf-01 for Gymnogongrus flabelliformis-ethanol, and Gf-02 for Gymnogongrus flabelliformis-acetone. Each bottle was filled with 100 mL of 96% ethanol and 96% acetone and stored at 25 °C for two weeks. The fine residue in the solution was separated using a vacuum filter, and the filtrate was used as dye without further purification.

#### 2.3 DSSC preparation

The DSSC anode was prepared by cleaning a  $2.5 \times 2.0 \text{ cm}^2$  piece of indium-tin-oxide (ITO) conductive glass with ethanol (Aldrich) for 15 minutes in an ultrasonic bath, followed by airdrying at room temperature. Using spin coating, titanium dioxide (TiO<sub>2</sub>) (Dyesol Co., Australia) was deposited onto the ITO conductive glass over a  $1.0 \text{ cm}^2$  area. After deposition, the glass was heated at  $120 \,^{\circ}\text{C}$  for 20 minutes and sintered at  $450 \,^{\circ}\text{C}$  for four hours in a furnace to solidify the TiO<sub>2</sub> layer. Once cooled to  $80 \,^{\circ}\text{C}$ , the TiO<sub>2</sub> was immersed in a dye solution and kept in the dark at room temperature for 24 hours to allow dye adhesion. Any impurities on the film were removed by washing with anhydrous ethanol and drying in moisture-free air.

In this study, an electrolyte solution was sandwiched between the  ${\rm TiO_2}$  film photoelectrode and a counter electrode made of reduced graphene oxide (rGO) (Prima, Rusliani, Suhendi, & Yuliarto, 2024). This counter electrode served as the cathode, regenerating the ions of the electrolytic element to create a solar cell. A standard liquid electrolyte (EL-141, Dyesol Co., Australia) was introduced into the sandwich cell. The electrolyte is crucial in charge transfer and neutralizing dye ions resulting from electron loss. The clamped-together electrodes were temporarily sealed with ovalbumin glue to prevent electrolyte leakage (Prima, Yuliarto, Suendo, & Suyatman, 2014).

#### 2.4 Characterization and Measurement

UV-vis spectrophotometry was employed to identify the chlorophyll pigments in Cl-01, Cl-02, Gf-01, and Gf-02. The pigments were diluted in a 1:1 ratio and analyzed using a UV 1600 PC spectrophotometer, measuring 400 to 800 nm wavelengths. This process ensured the accurate assessment of the dye solution's optical properties when bound to the TiO<sub>2</sub> layer. For Fourier Transform Infrared (FTIR) spectroscopy, the crude extracts were finely ground with potassium bromide (KBr) to produce powder samples. These samples were then compressed into pellets using a 10-ton hydraulic press, creating transparent specimens that allowed infrared radiation to pass through. The FTIR spectra were recorded using a Shimadzu FTIR Prestige 21 spectrophotometer over a spectral range of 400 cm<sup>-1</sup> to 4500 cm<sup>-1</sup>.

Cyclic voltammetry (C-V) measurements were performed to determine the oxidation and reduction potential of the dye solution. These measurements were conducted using an eDAQ potentiostat equipped with an e-coder 401 and Echem software, within a range of -1.8 mV to +1.8 mV, in a positive initial direction. A three-electrode system was employed, consisting of a glassy carbon working electrode, a platinum counter electrode, and an Ag/AgCl reference electrode in a 0.1 M KNO<sub>3</sub> solution. The dye solution was prepared by mixing 0.5 mL of dye extract with 10 mL of 0.1 M KNO<sub>3</sub>. (Adedokun, Sanusi, & Awodugba, 2018). The C-V measurement results were used to determine the HOMO-LUMO energy levels and redox potential gap using equations (1) to (3) (Shafiee, Salleh, & Yahaya, 2011)

$$HOMO = - (Eox + 4,4)$$
(1)

 $LUMO = - (Ered + 4,4)$  (2)

$$Eg = HOMO - LUMO$$
 (3)

To analyze the J-V characteristics, a 100 mW/cm² AM 1.5 solar simulator was utilized to measure the short-circuit photocurrent (Jsc) and open-circuit voltage (Voc) (Han, Koide, Chiba, & Mitate, 2004). The J-V curves also provided values for Vmax, Jmax, fill factor (FF), and efficiency ( $\eta$ ), key indicators of the solar cell's power output. (Prima  $et\ al.$ , 2024). The irradiance in the ambient environment was measured using a precision spectral pyranometer (MS-402F, Eiko-Seiki, Japan), ensuring an illumination intensity of 100 mW/cm², generated by a 500-watt Philips Xenon lamp. The fill factor (FF) and efficiency ( $\eta$ ) of the dye-sensitized solar cell (DSSC) were calculated using equations (4) and (5).

$$FF = \frac{J_{max}.V_{max}}{J_{sc.V_{OC}}}$$
 (4)

$$\eta = \frac{J_{sc}.V_{oc}}{P_{in}} x FF$$
 (5)

#### 3. Results and Discussions

#### 3.1 SEM Characterization Analysis

Surface morphology of the TiO<sub>2</sub> layer is ascertained by SEM characterization. Small, uniformly sized particles with a 64 nm size define the surface of the mesoporous TiO<sub>2</sub> layer according to SEM results shown in Figure 2 (Prima *et al.*, 2024). Using the Scherrer equation, ImageJ program verified the mesoporous

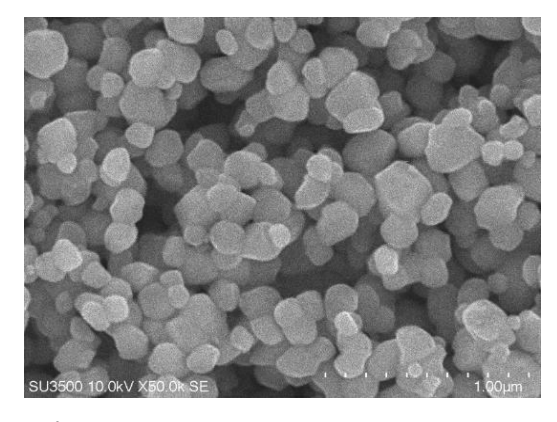
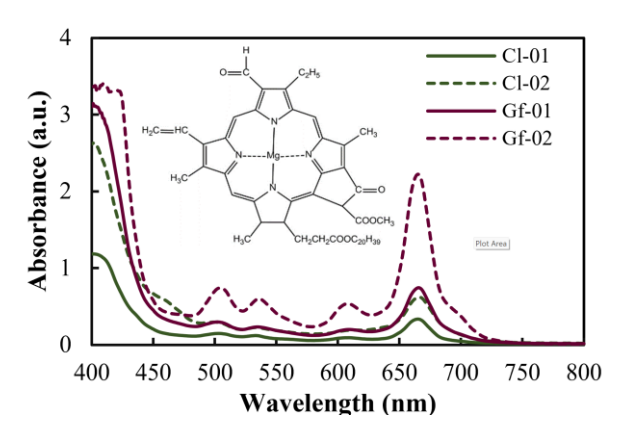


Fig 2. Morphology of the TiO<sub>2</sub> layer by SEM analysis

morphological grain size, which matched earlier estimates. Particularly, the small and homogeneous grain size helps to lower the aggregate, so lowering the dye adsorbed on TiO2. Concurrently, the dye absorption capacity of the nanoparticles on TiO<sub>2</sub> surface can be raised by their crystal structure. Apart from the cavity, the thickness of the TiO2 surface layer can influence the dye molecule absorption. The thickness of TiO<sub>2</sub> used in this work was 9.1 µm; this value corresponds with the normal thickness for  $TiO_2$  thin films, which is 7-20  $\mu m$ (Trihutomo et al., 2019). The electron diffusion path is faster since the variation reduces the relevance of the interconnection between particles. Although the thickness of the TiO<sub>2</sub> layer is not ideal, in this work the thin TiO<sub>2</sub> photoelectrode has a consistent and hollow grain structure that lets electrons migrate fast and improves the DSSC's performance. Thus, the quick electron diffusion process can help DSSC to perform better.

#### 3.2 UV-Vis Absorption Spectra of Chlorophyll Pigment

Dyes serve as key sensitizers in DSSCs, enabling sunlight absorption and converting solar energy into electrical energy. Many metal complexes and organic dyes have been synthesized and used as sensitizers. Among natural dyes, chlorophyllfound in macroalgae—is essential for photosynthetic organisms, including higher plants, algae, and cyanobacteria (Orona-Navar et al., 2021; Tanaka & Tanaka, 2011). During photosynthesis, it is critical for light absorption, electron transfer, and primary charge separation (Koyama, Miki, Wang, & Nagae, 2009). An absorption spectrophotometer measures the intensity of light absorbed as a function of wavelength. The absorption spectrum of macroalgae dye extracts indicates the chlorophyll pigment content in Cl-01, Cl-02, Gf-01, and Gf-02. Figure 3 illustrates the light absorption spectrum across a wide range of visible to nearinfrared wavelengths (400-800 nm). As shown in Figure 2, the four sample extract solutions exhibit a similar graphical shape despite variations in energy absorption values. These differences in energy absorption are attributed to variations in the concentrations of each solution. The energy absorption of a compound at a specific wavelength increases with the number of molecules undergoing a transition. This absorption depends on the electronic structure of the compound, its concentration, and the material's cell length. For example, the dye from Cl-01 exhibits two prominent absorption peaks at 402 nm and 666 nm. In comparison, the dye from Cl-02 also shows two prominent peaks at 402 nm and 665 nm, indicating chlorophyll pigments. Additionally, two significant peaks indicating chlorophyll pigments appear at wavelengths of 401 nm and 666 nm, 403 nm and 665 nm, and several low-intensity peaks in both Gf-01 and



**Fig 3**. UV-Vis Absorption Spectra of Chlorophyll from *Caulerpa racemosa* (Cl-01;Cl-02) and *Gymnogongrus flabelliformis* (Gf-01;Gf-02)

Gf-02 extracts. The wavelength and intensity of each absorption peak usually reflect the transition energy and the transition-dipole moment in the base-to-Soret transition state. Using algal pigments as dyes for DSSCs presents an attractive option for low-cost cell production. Furthermore, chlorophyll extracted from these species provides additional environmental benefits.

#### 3.3 Extracted dye FTIR analysis

In addition to UV-Vis spectrophotometry, FTIR was also used to analyze the light absorption characteristics of chlorophyll dyes. The functional groups of the chemically active compounds in the four macroalgae extract samples were identified based on their peak values in the infrared radiation region. Figure 4 and Table 1 present the Fourier Transform Infrared (FTIR) spectra of dye-extracted pigments from Caulerpa racemosa (Cl-01, Cl-02) and Gymnogongrus flabelliformis (Gf-01, Gf-02). The FTIR spectra for Cl-01 and Cl-02 exhibit vibrations at wave numbers 3400 cm<sup>-1</sup> and 3402 cm<sup>-1</sup>, respectively, which are nearly identical. However, these values differ from those of Gf-01 and Gf-02, recorded at 3425 cm<sup>-1</sup> and 3379 cm<sup>-1</sup>, respectively. The observed vibrations correspond to the O-H functional group (Cheng, Yang, Liu, Liu, & Fan, 2023; Greco, Varon, & Iorio, 2022). This difference may be due to the interaction of water molecules with the C=O groups in esters and keto compounds. All extract samples exhibited C-H hydrocarbon groups on the phytol chain at 2933 cm<sup>-1</sup>, 2949 cm<sup>-1</sup>, 2960 cm<sup>-1</sup>, and 2945 cm<sup>-1</sup>, respectively. (Namie, Kim, &

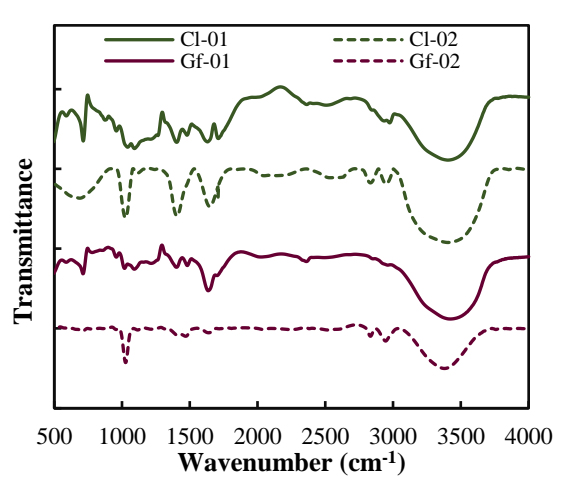


Fig 4. FTIR Spectrum of dye extract

1050-1000

**Table 1**The Vibrational absorption wavelengths of chlorophyll functional groups based on ET-IR spectra

C-O

Commis	Functional Group	Wavelength (cm <sup>-1</sup> )		
Sample		Chlorophyll Extract	Reference	
Caulerpa racemosa				
Cl-01 ; Cl-02	О-Н	3402; 3400	3570-3200	
	C-H (alkane)	2933 ; 2949	2970-2815	
	C=O (Ester)	1710 ; -	1750-1700	
	C=O (Keto)	1631 ; 1647	1650-1600	
	C=C (Aromatic)	1479 ; -	1510-1450	
	C=N	1265 ; -	1380-1250	
	C-O	1041; 1024	1050-1000	
Gymnogongrus flabelliformis				
Gf-01; Gf-02	О-Н	3425; 3379	3570-3200	
	C-H (alkane)	2960 ; 2945	2970-2815	
	C=O (Ester)	1701 ; -	1750-1700	
	C=O (Keto)	1635 ; 1631	1650-1600	
	C=C (Aromatic)	1483 ; 1465	1510-1450	
	C=N	-	1380-1250	

1018; 1026

Yonezawa, 2023). Strong peaks at 1710 cm<sup>-1</sup> and 1701 cm<sup>-1</sup> indicate vibrations of the C=O group of the ester in Cl-01 and Gf-01 (Endo et al., 2017), whereas Cl-02 and Gf-02 exhibited no vibrations of the C=O ester group. Bending vibrations in Cl-01, Gf-01, and Cl-02 were captured with high intensity at wavenumbers 1631 cm<sup>-1</sup>, 1635 cm<sup>-1</sup>, and 1647 cm<sup>-1</sup>, respectively, which demonstrated the presence of C=O keto groups (Dedeepya et al., 2022); while the aromatic C=C group in Cl-01 and Gf-01 exhibited in the peaks at 1479 cm<sup>-1</sup> and 1483 cm<sup>-1</sup>. In addition, the absorption peak at 1265 cm-1 refers to the vibration of the C=N group, which is exclusively found in the Cl-01 extract. Furthermore, absorption peaks indicating C-O vibrations were found in all samples with wavenumbers at 1041 cm<sup>-1</sup> and 1024 cm<sup>-1</sup> for Cl-01 and Cl-02, respectively, while in Gf-01 and Gf-02, the wavenumbers were 1018 cm<sup>-1</sup> and 1026 cm<sup>-1</sup>, respectively (Chang *et al.*,2013).

#### 3.4 Cyclic voltammetry characterization

Figure 5 illustrates the reduction-oxidation reaction of the dye, characterized using cyclic voltammetry. The analyzed energies include reduction energy ( $E_{red}$ ) and oxidation energy ( $E_{oks}$ ), which are then converted into HOMO (highest occupied molecular orbital) and LUMO (lowest unoccupied molecular orbital) energy levels. Oxidation energy represents the energy

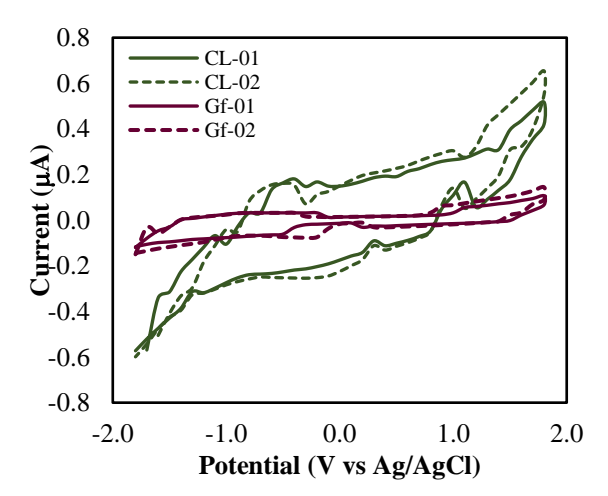


Fig 5. Cyclic Voltammetry Curve of Dye Extract

required for a molecule to release electrons, while reduction energy indicates the energy needed to gain electrons. HOMO acts as an electron donor because it is the outermost orbital (highest energy) containing at least one electron. In contrast, LUMO serves as an electron acceptor, as it is the lowest energy orbital with available space to receive electrons. The oxidation process of the dye molecule occurs at the anodic potential and returns to its original state after the reduction step. Due to its irreversible nature, the dye molecule attaches to the TiO2 surface and completely transforms after oxidation. (Pal & Rahaman, 2015). For optimal efficiency in the electron transport cycle, the HOMO energy level must be more positive than the conduction band of the working electrode (Kumar & Rao 2017). energetic properties influence the redox reaction characteristics of the dye and depend on the solvent used. The solvent affects the surface charge density and the presence of dipoles at various interfaces between TiO<sub>2</sub>, the dye, and the electrolyte.

The results of the cyclic voltammetry assays performed on each dye sample are shown in Table 2, which highlights the differences in LUMO and HOMO energy levels. Based on the data presented in Table 2, the energy gaps of the two macroalgae species are not significantly different. This is due to the extraction process of the four samples using the same solvents, namely acetone and ethanol. Due to electronegative OH groups, ethanol is a polar molecule that can bond with the dissolved molecules. In contrast, acetone is a polar solvent, exhibiting both polar and non-polar properties because of the C=O and C-CH<sub>2</sub> bonds. This implies that the stability of the dye molecules is maintained by both ethanol and acetone (Katritzky et al., 2004). The gap energies of the chlorophyll pigments in Cl-01, Cl-02, Gf-01, and Gf-02 are 2.4 eV, 2.3 eV, 1.4 eV, and 1.3 eV, respectively. Gymnogongrus flabelliformis samples (Gf-01; Gf-02) demonstrate better energy gaps than Caulerpa racemosa samples (Cl-01; Cl-02). This is due to the lifetime length of absorbed photon energy and the broader absorbance spectrum, which leads to a higher current and a greater number of excited electrons (Prabavathy et al., 2017).

A broad band gap enhances electron transition from the conduction band to the valence band, expanding the photocatalytic reaction space and increasing dye absorption. This results in a broader spectrum of color absorption. As a result, the extraction of chlorophyll dye generated from *Caulerpa racemosa* and *Gymnogongrus flabelliformis* may function as a photosensitizer for dye-sensitized solar cells (DSSC),

Table 2
Cyclic Voltammetry Result of Dyes

Cyclic Voltammetry Result of Dyes							
Sample	E <sub>oks</sub> (eV)	$E_{red}$ (eV)	HOMO (eV)	LUMO (eV)	Eg (eV)		
Cl-01	1.3	-1.10	-5.70	-3.30	2.4		
Cl-02	1.1	-1.20	-5.50	-3.20	2.3		
Gf-01	8.0	-0.60	-5.20	-3.80	1.4		
Gf-02	0.6	-0.70	-5.00	-3.70	1.3		

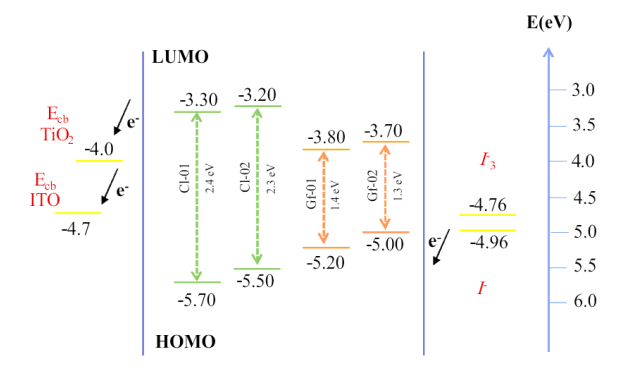


Fig 6. DSSC Energy Level Diagram of dye extract

because its LUMO potential energy is more negative than the conduction band of  $\mathrm{TiO_2}$  (-4.00 eV). In comparison, its HOMO potential energy is more positive than the redox energy of the electrolyte (-4.96 eV), as illustrated in Figure 6. This alignment directly affects the values of electric current density ( $\mathit{Jsc}$ ) and open-circuit voltage ( $\mathit{Voc}$ ).

## 3.5 DSSC performance of Dye Pigment from Caulerpa racemose and Gymnogongrus flabelliformis

Figure 7 presents experimental data on the DSSC performance of dye pigments extracted from macroalgae, characterizing the acquired J-V curve in terms of short-circuit density (Jsc), open-circuit voltage (Voc), fill factor (FF), and power conversion efficiency (n), as detailed in Table 3. The chlorophyll pigments extracted from Caulerpa racemosa (Cl-01; Cl-02) and Gymnogongrus flabelliformis (Gf-01; Gf-02) exhibited lower efficiencies compared to previously reported values for other macroalgae species. The maximum efficiency recorded in this study was 0.020%, which is lower than the efficiencies reported in studies using chlorophyll extracts from other macroalgae. Table 3 confirms this finding, showing that DSSCs made from Undaria pinnatifida and Ulva intestinalis achieved efficiencies of 0.36% (Minicante et al., 2016) and 0.13% (Dumbrava et al., 2016). Several factors, including the thickness of anatase TiO2 on the ITO conductivity glass surface, may contribute to this discrepancy. As the TiO2 layer thickens, transmittance decreases, reducing the dye's ability to absorb light (Kao, Chen, Young, Kung, & Lin, 2009). Moreover, an effective and efficient natural dye for DSSCs must meet several criteria. These include a hydrophobic surface, an absorption spectrum covering both visible light and the near-infrared region, and localization of the LUMO near the anchoring group connecting the dye and the TiO2 molecule. And also a HOMO energy level lower than that of the redox mediator, localization of the positive charge generated post-electron transfer away

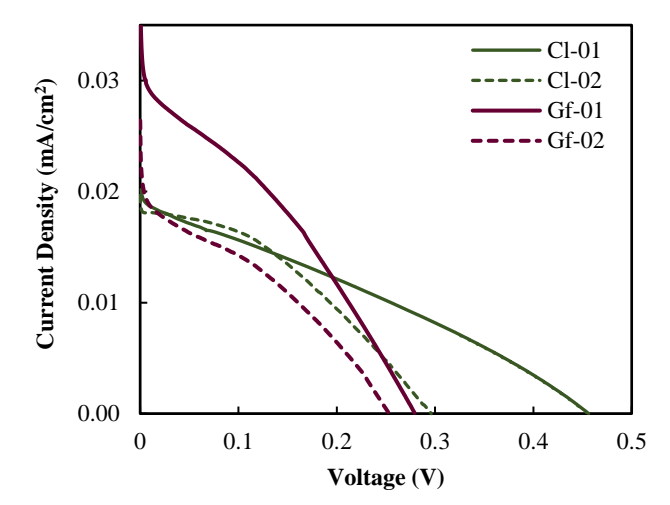


Fig 7. DSSC performance of dye extract

from the TiO2 surface (donor region), and the absence of aggregate formation on the TiO2 surface (Mishra, Fischer, & Bäuerle, 2009). These aspects affected the amount of excitons produced and the total number of charges that extended to the electrode when irradiation occurred. An extensive route of charge diffusion may trigger recombination of numerous charges before reaching the electrode, consequently decreasing the efficiency (Gong, Liang, & Sumathy, 2012). Even though the present research indicate results of this certain drawbacks/limitations/weaknesses compared to previous studies utilizing other species of macroalgae, generating natural dye from the designated species of Caulerpa racemosa and Gymnogongrus flabelliformis has not been previously documented. Further investigation may lead to significant improvements in DSSC performance.

Figure 8 shows the relationship between photopower and photovoltage (PV) for the DSSC using dyes taken from the macroalgae *Caulerpa racemose* and *Gymnogongrus flabelliformis*. These curves were used to calculate the maximum power ( $P_{max}$ ) and maximum potential ( $V_{max}$ ) values. The  $P_{max}$  values obtained from *Caulerpa racemose* macroalgae extracts Cl-01 and Cl-02 were 0.2606 mW/cm² and 0.1706 mW/cm², respectively. While, the  $P_{max}$  values for *Gymnogongrus flabelliformis* extracts were 0.1631 mW/cm² for Gf-01 and 0.1501 mW/cm² for Gf-02, respectively.

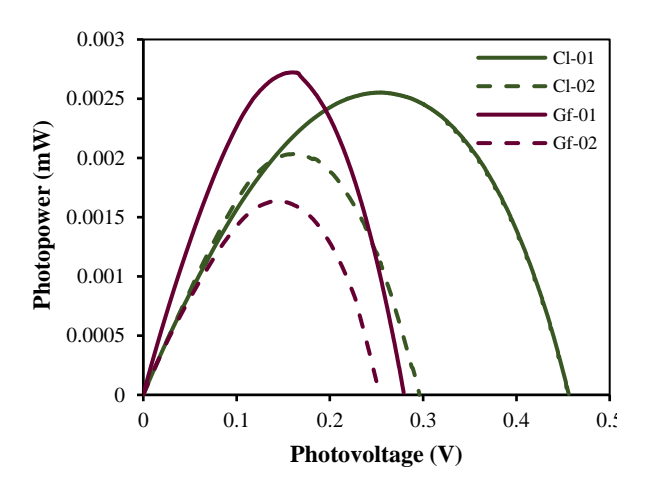


Fig 8. Photopower-photovoltage Curve of dye extract

**Table 3**The Sensitized DSSCs performance of various natural dyes from macroalgae

Voc FF (%) Counter electrode Electrolyte Reference Sample η (%) (mA/cm2) (V) 24.45 0.019 Caulerpa racemose-01 0.023 0.46 rGO Liquid 0.015 0.020 0.30 34.95 rGO Liquid Caulerpa racemose-02 Gymnogongrus flabelliformis-01 0.041 0.28 23.89 0.020 rGO Liquid Gymnogongrus flabelliformis-02 0.026 24.49 0.012 rGO Liquid 0.25 U. pinnatifida 0.8 0.36 0.69 0.178 Pt Liquid (Calogero et al., 2014) U. pinnatifida 0.99 0.52 0.71 0.36 Pt Liquid (Minicante et al., 2016) Ulva intestinalis Linnaeus Pt 0.38 0.58 0.46 0.13 Liquid (Dumbrava et al., 2016) Pithophora roettleri 1.25 0.35 Carbon-coated Cu Quasi-solid (Chatterjee et al, 2024) 0.59 0.0001 0.24 0.48 Carbon black (Wei et al., 2019) Manihot esculenta sp Cladophora green 0.145 0.58 0.59 0.055 Pt (Lim et al., 2015)

#### 4. Conclusion

The chlorophyll extract obtained from Caulerpa racemosa and Gymnogongrus flabelliformis serves as a sensitizer in DSSCs. Based on the research data, the UV-Vis and FTIR results confirm that the extracted chlorophyll pigments possess the necessary chemical and physical characteristics for DSSC applications. Additionally, the two-macroalgae species exhibit different HOMO/LUMO gap energy values, with Caulerpa racemosa showing gap energy values of 2.4 eV and 2.3 eV, while Gymnogongrus flabelliformis has gap energy values of 1.4 eV and 1.3 eV. The performance efficiency of the DSSC was 0.019% and 0.015% for Caulerpa racemosa and 0.020% and 0.012% for Gymnogongrus flabelliformis, respectively. Therefore, utilizing pigments from these two macroalgae species from Maluku waters as photosensitizers has the potential to enhance DSSC performance in the future, given their accessibility, affordability, biodegradability, and environmental friendliness.

#### Acknowledgments

This research is supported by Lembaga Pengelola Dana Pendidikan (LPDP) of the Indonesian Ministry of Finance with the scholarship number 202108212007478. This research also is partialy supported by Penelitian Terapan Unggulan Perguruan Tinggi, Direktorat Jenderal Pendidikan Tinggi (1269 /UN40.LP/PT.01.03/2024)

**Author Contributions**: Semuel Unwakoly and Eka Cahya Prima.: Conception, research design, analysis and interpretation, research draft composition, Liliasari; research supervision and mentorship, project management and organization, Heli S. H. Munawaroh; Project reviewer, editor and validator, Sri Hartati and Arramel; review and editing. Prima Fitri Ruslian: C-V analysis. The authors have approved the issued manuscript.

**Funding:** LPDP Scholarship of the Indonesian Ministry of Finance funded this present study.

**Conflicts of Interest:** This is an affirmation that the authors have no both competing financial and personal interests that affect the work in the reported paper.

#### References

- Adedokun, O., Sanusi, Y. K., & Awodugba, A. O. (2018). Solvent dependent natural dye extraction and its sensitization effect for dye sensitized solar cells. *Optik*, 174, 497-507. https://doi.org/10.1016/j.ijleo.2018.06.064
- Calogero, G., Citro, I., Di Marco, G., Minicante, S. A., Morabito, M., & Genovese, G. (2014). Brown seaweed pigment as a dye source for

- photoelectrochemical solar cells. *Spectrochimica Acta Part A: Molecular and Biomolecular Spectroscopy, 117*, 702-706. https://doi.org/10.1016/j.saa.2013.09.019
- Chang, H., Kao, M. J., Chen, T. L., Chen, C. H., Cho, K. C., & Lai, X. R. (2013). Characterization of natural dye extracted from wormwood and purple cabbage for dye-sensitized solar cells. International Journal of Photoenergy, 2013(1), 159502. https://doi.org/10.1155/2013/159502
- Chatterjee, A., Kathirvel, A., Manivasagam, T. G., & Batabyal, S. K. (2024). Sustainable power generation from live freshwater photosynthetic filamentous macroalgae Pithophora. *Journal of Science: Advanced Materials and Devices*, 9(2), 100674. https://doi.org/10.1016/j.jsamd.2024.100674
- Chen, J. K., Wang, M.-Y., Chen, Y.-R., & Chen, Y.-s. (2012). Exploring knowledge flows of network on patent of dye sensitized solar cell.

  Paper presented at the 2012 Proceedings of PICMET'12: Technology Management for Emerging Technologies.
- Cheng, P., Yang, L., Liu, Y., Liu, J., & Fan, Y. (2023). Promotion of sugar extraction from sewage sludge by microwave combined with thermal-alkaline pretreatment. *Water*, *15*(7), 1291. https://doi.org/10.3390/w15071291
- Ciani, L., Catelani, M., Carnevale, E. A., Donati, L., & Bruzzi, M. (2014).

  Evaluation of the aging process of dye-sensitized solar cells under different stress conditions. *IEEE Transactions on Instrumentation and Measurement*, 64(5), 1179-1187. https://doi.org/10.1109/TIM.2014.2381352
- Cui, Y., Xu, Y., Yao, H., Bi, P., Hong, L., Zhang, J., . . . Ren, J. (2021).

  Single-junction organic photovoltaic cell with 19% efficiency.

  Advanced Materials, 33(41), 2102420.

  https://doi.org/10.1002/adma.202102420
- Davies, K. (2004). *Plant Pigments and Their Manipulation; Annual Plant Reviews* (Vol. 14): Blackwell Publishing Ltd. https://doi.org/10.1093/aob/mci287
- Dedeepya, G., Shanmugan, S., Sundari, G. S., Devi, N. L., Meenachi, M., Kiran, M. G., & Selvaraju, P. (2022). Dyes prepared from leaf extract of siriyanangai (Andrographis Paniculata) with the effect of TiO2 based DSSCs. *Materials Today: Proceedings, 66*, 3644-3650. https://doi.org/10.1016/j.matpr.2022.07.188
- Dumbrava, A., Lungu, J., & Ion, A. (2016). Green seaweeds extract as co-sensitizer for dye sensitized solar cells. *Scientific Study & Research. Chemistry & Chemical Engineering, Biotechnology, Food Industry,* 17(1), 13. https://pubs.ub.ro/dwnl.php?id=CSCC6201601V01S01A0002
- Endo, T., Reddy, L., Nishikawa, H., Kaneko, S., Nakamura, Y., & Endo, K. (2017). Composite engineering–direct bonding of plastic PET films by plasma irradiation. *Procedia Engineering*, 171, 88-103. https://doi.org/10.1016/j.proeng.2017.01.315
- Erdogdu, M., Atilgan, A., Erdogdu, Y., & Yildiz, A. (2024). Flavonoid from Hedera helix fruits: A promising new natural sensitizer for DSSCs. *Journal of Photochemistry and Photobiology A: Chemistry,* 448, 115288. https://doi.org/10.1016/j.jphotochem.2023.115288
- Ferreira, F., Babu, R. S., de Barros, A., Raja, S., da Conceição, L., & Mattoso, L. (2020). Photoelectric performance evaluation of DSSCs using the dye extracted from different color petals of Leucanthemum vulgare flowers as novel sensitizers. Spectrochimica Acta Part A: Molecular and Biomolecular

- *Spectroscopy,* 233, 118198. https://doi.org/10.1016/j.saa.2020.118198
- Gong, J., Liang, J., & Sumathy, K. (2012). Review on dye-sensitized solar cells (DSSCs): Fundamental concepts and novel materials. *Renewable and Sustainable Energy Reviews*, 16(8), 5848-5860. https://doi.org/10.1016/j.rser.2012.04.044
- Grätzel, M. (2001). Photoelectrochemical cells. *Nature*, 414(6861), 338-344. https://doi.org/10.1038/35104607
- Greco, I., Varon, C., & Iorio, C. S. (2022). Synthesis and Characterization of a new Alginate-Gelatine Aerogel for Tissue Engineering. Paper presented at the 2022 44th Annual International Conference of the IEEE Engineering in Medicine & Biology Society (EMBC). https://doi.org/10.1109/EMBC48229.2022.9871508
- Grimm, B., Porra, R. J., Rüdiger, W., & Scheer, H. (2006). Chlorophylls and Bacteriochlorophylls (Advances in Photosynthesis and Respiration). Advances in Photosynthesis and Respiration. https://doi.org/10.1007/1-4020-4516-6
- Han, L., Koide, N., Chiba, Y., & Mitate, T. (2004). Modeling of an equivalent circuit for dye-sensitized solar cells. *Applied Physics Letters*, 84(13), 2433-2435. https://doi.org/10.1063/1.1690495
- Hao, S., Wu, J., Huang, Y., & Lin, J. (2006). Natural dyes as photosensitizers for dye-sensitized solar cell. *Solar Energy*, 80(2), 209-214. https://doi.org/10.1016/j.solener.2005.05.009
- Iqbal, M. Z., Ali, S. R., & Khan, S. (2019). Progress in dye sensitized solar cell by incorporating natural photosensitizers. *Solar Energy*, 181, 490-509. https://doi.org/10.1016/j.solener.2019.02.023
- Kao, M., Chen, H., Young, S., Kung, C., & Lin, C. (2009). The effects of the thickness of TiO2 films on the performance of dye-sensitized solar cells. *Thin solid films*, 517(17), 5096-5099. https://doi.org/10.1016/j.tsf.2009.03.102
- Katritzky, A. R., Fara, D. C., Yang, H., Tämm, K., Tamm, T., & Karelson, M. (2004). Quantitative measures of solvent polarity. *Chemical reviews*, 104(1), 175-198. https://doi.org/10.1021/cr020750m
- Koyama, Y., Miki, T., Wang, X.-F., & Nagae, H. (2009). Dye-sensitized solar cells based on the principles and materials of photosynthesis: mechanisms of suppression and enhancement of photocurrent and conversion efficiency. *International journal of molecular sciences, 10*(11), 4575-4622. https://doi.org/10.3390/ijms10114575
- Kumar, Á., & Kandpal, T. C. (2007). Renewable energy technologies for irrigation water pumping in India: A preliminary attempt towards potential estimation. *Energy*, *32*(5), 861-870. https://doi.org/10.1016/j.energy.2006.05.004
- Kumar, S. G., & Rao, K. K. (2017). Comparison of modification strategies towards enhanced charge carrier separation and photocatalytic degradation activity of metal oxide semiconductors (TiO2, WO3 and ZnO). Applied Surface Science, 391, 124-148. https://doi.org/10.1016/j.apsusc.2016.07.081
- Kumara, N., Lim, A., Lim, C. M., Petra, M. I., & Ekanayake, P. (2017).
  Recent progress and utilization of natural pigments in dye sensitized solar cells: A review. *Renewable and Sustainable Energy Reviews*, 78, 301-317. https://doi.org/10.1016/j.rser.2017.04.075
- Liline, S., Rumahlatu, D., Zubaidah, S., Salmanu, S., & Sangur, K. (2024).

  Influence of physicochemical environmental factors on morphometric characteristics of macroalgae from Ambon Island, Indonesia. *Biodiversitas Journal of Biological Diversity*, 25(4). https://doi.org/10.13057/biodiv/d250412
- Lim, A., Haji Manaf, N., Tennakoon, K., Chandrakanthi, R., Lim, L. B. L., Bandara, J., & Ekanayake, P. (2015). Higher performance of DSSC with dyes from Cladophora sp. as mixed cosensitizer through synergistic effect. *Journal of Biophysics*, 2015. https://doi.org/10.1155/2015/510467
- Mandal, R., & Dutta, G. (2020). From photosynthesis to biosensing: Chlorophyll proves to be a versatile molecule. *Sensors International*, 1, 100058. https://doi.org/10.1016/j.sintl.2020.100058
- Minicante, S. A., Ambrosi, E., Back, M., Barichello, J., Cattaruzza, E., Gonella, F., . . . Trave, E. (2016). Development of an eco-protocol for seaweed chlorophylls extraction and possible applications in dye sensitized solar cells. *Journal of Physics D: Applied Physics*, 49(29), 295601. https://doi.org/10.1088/0022-3727/49/29/295601
- Mishra, A., Fischer, M. K., & Bäuerle, P. (2009). Metal-free organic dyes for dye-sensitized solar cells: From structure: Property

- relationships to design rules. *Angewandte Chemie International Edition,* 48(14), 2474-2499. https://doi.org/10.1002/anie.200804709
- Namie, M., Kim, J.-H., & Yonezawa, S. (2023). Enhanced Dyeing of Polypropylene Using Fluorine–Oxygen Gas Mixtures. *Colorants*, 2(3), 552-564. https://doi.org/10.3390/colorants2030027
- Olea, A., Ponce, G., & Sebastian, P. (1999). Electron transfer via organic dyes for solar conversion. *Solar energy materials and solar cells*, 59(1-2), 137-143. https://doi.org/10.1016/S0927-0248(99)00038-0
- Orona-Navar, A., Aguilar-Hernández, I., Nigam, K., Cerdán-Pasarán, A., & Ornelas-Soto, N. (2021). Alternative sources of natural pigments for dye-sensitized solar cells: Algae, cyanobacteria, bacteria, archaea and fungi. *Journal of Biotechnology, 332*, 29-53. https://doi.org/10.1016/j.jbiotec.2021.03.013
- Pal, K., & Rahaman, C. H. (2015). Phytochemical and antioxidant studies of Justicia gendarussa Burm. F. an ethnomedicinal plant. *Int. J. Pharm. Sci*, 6, 3454-3462. https://doi.org/10.13040/IJPSR.0975-8232.6(8).3454-62
- Prabavathy, N., Shalini, S., Balasundaraprabhu, R., Velauthapillai, D., Prasanna, S., & Muthukumarasamy, N. (2017). Enhancement in the photostability of natural dyes for dye-sensitized solar cell (DSSC) applications: a review. *International Journal of Energy Research*, 41(10), 1372-1396. https://doi.org/10.1002/er.3703
- Prima, E. C., Nugroho, H. S., Refantero, G., Panatarani, C., & Yuliarto, B. (2020). Performance of the dye-sensitized quasi-solid state solar cell with combined anthocyanin-ruthenium photosensitizer. *RSC advances*, 10(60), 36873-36886. https://doi.org/10.1039/D0RA06550A
- Prima, E. C., Rusliani, P. F., Suhendi, E., & Yuliarto, B. (2024).

  Performance of dye-sensitized solar cells with mixed three natural pigments and reduced graphene oxide as a counter electrode.

  Results in Optics, 14, 100592. https://doi.org/10.1016/j.rio.2023.100592
- Prima, E. C., Yuliarto, B., Suendo, V., & Suyatman. (2014). Improving photochemical properties of Ipomea pescaprae, Imperata cylindrica (L.) Beauv, and Paspalum conjugatum Berg as photosensitizers for dye sensitized solar cells. *Journal of Materials Science: Materials in Electronics, 25*, 4603-4611. https://doi.org/10.1007/s10854-014-2210-x
- Richhariya, G., Kumar, A., Tekasakul, P., & Gupta, B. (2017). Natural dyes for dye sensitized solar cell: A review. *Renewable and Sustainable Energy Reviews*, 69, 705-718. https://doi.org/10.1016/j.rser.2016.11.198
- Ruba, N., Prakash, P., Sowmya, S., Janarthana, B., Prabu, A. N., Chandrasekaran, J., . . . Yahia, I. (2021). Recent advancement in photo-anode, dye and counter cathode in dye-sensitized solar cell: a review. *Journal of Inorganic and Organometallic Polymers and Materials*, 31, 1894-1901. https://doi.org/10.1007/s10904-020-01854-6
- Shafiee, A., Salleh, M. M., & Yahaya, M. (2011). Determination of HOMO and LUMO of [6, 6]-phenyl C61-butyric acid 3-ethylthiophene ester and poly (3-octyl-thiophene-2, 5-diyl) through voltametry characterization. *Sains Malaysiana*, 40(2), 173-176. https://doi.org/10.4028/www.scientific.net/SSP.307.207
- Tanaka, R., & Tanaka, A. (2011). Chlorophyll cycle regulates the construction and destruction of the light-harvesting complexes. *Biochimica et Biophysica Acta (BBA)-Bioenergetics*, 1807(8), 968-976. https://doi.org/10.1016/j.bbabio.2011.01.002
- Trihutomo, P., Soeparman, S., Widhiyanuriyawan, D., & Yuliati, L. (2019). Performance Improvement of Dye-Sensitized Solar Cell-(DSSC-) Based Natural Dyes by Clathrin Protein. *International Journal of Photoenergy*, 2019(1), 4384728. https://doi.org/10.1155/2019/4384728
- Ubani, C., Ibrahim, M., Teridi, M., Sopian, K., Ali, J., & Chaudhary, K. (2016). Application of graphene in dye and quantum dots sensitized solar cell. *Solar Energy*, 137, 531-550. https://doi.org/10.1016/j.solener.2016.08.055
- Venugopal, G., Krishnamoorthy, K., & Kim, S.-J. (2013). An investigation on high-temperature electrical transport properties of graphene-oxide nano-thinfilms. *Applied surface science, 280*, 903-908. https://doi.org/10.1016/j.apsusc.2013.05.089
- Wang, X.-F., Zhan, C.-H., Maoka, T., Wada, Y., & Koyama, Y. (2007). Fabrication of dye-sensitized solar cells using chlorophylls c1 and

- c2 and their oxidized forms c1' and c2' from Undaria pinnatifida (Wakame). *Chemical physics letters, 447*(1-3), 79-85. https://doi.org/10.1016/j.cplett.2007.08.097
- Wei, Q. S., Aizat, M. F., Diyanti, A., Ishak, W. M. F., Salleh, H., Wong, K. N. S. W. S., & Adli, H. K. (2019). Kappaphycus alvarezii sp., Sargassum polycystum sp. and Manihot esculenta sp. as photosensitizers in dye-sensitized solar cells. Paper presented at the AIP Conference Proceedings. https://doi.org/10.1063/1.5089327
- Wu, M., & Ma, T. (2014). Recent progress of counter electrode catalysts in dye-sensitized solar cells. *The Journal of Physical Chemistry C, 118*(30), 16727-16742. https://doi.org/10.1021/jp412713h
- Zhu, Y., Guo, H., Zheng, H., Lin, Y.-n., Gao, C., Han, Q., & Wu, M. (2016). Choose a reasonable counter electrode catalyst toward a fixed redox couple in dye-sensitized solar cells. *Nano Energy, 21*, 1-18. https://doi.org/10.1016/j.nanoen.2016.01.001



© 2025. The Author(s). This article is an open access article distributed under the terms and conditions of the Creative Commons Attribution-ShareAlike 4.0 (CC BY-SA) International License (http://creativecommons.org/licenses/by-sa/4.0/)